Transplanted enteric neural stem cells integrate within the developing chick spinal cord: implications for spinal cord repair

Running title: ENSC integrate within the chick embryo spinal cord

Benjamin Jevans[1], Conor J. McCann[1], Nikhil Thapar[1] and Alan J. Burns[1,2,3,4]

[1]Stem Cells and Regenerative Medicine, UCL Great Ormond Street Institute of Child Health, London, UK

[2]Department of Clinical Genetics, Erasmus Medical Center, Rotterdam, The Netherlands

[3]Current address: Gastrointestinal Drug Discovery Unit, Takeda Pharmaceuticals International, Cambridge, USA

[4]Corresponding author:
Alan J. Burns
Stem Cells and Regenerative Medicine,
UCL Great Ormond Street Institute of Child Health,
30 Guilford Street,
London,
WC1N 1EH,
UK
Tel. +1 617 551 8763
Email alan.burns@ucl.ac.uk

Abstract

Spinal cord injury (SCI) causes paralysis, multisystem impairment and reduced life expectancy, as yet with no cure. Stem cell therapy can potentially replace lost neurons, promote axonal regeneration and limit scar formation, but an optimal stem cell source has yet to be found. Enteric neural stem cells (ENSCs) isolated from the enteric nervous system (ENS) of the gastrointestinal (GI) tract are an attractive source. Here, we used the chick embryo to assess the potential of ENSCs to integrate within the developing spinal cord. *In vitro*, isolated ENSCs formed extensive cell connections when co-cultured with spinal cord (SC)-derived cells. Further, qRT-PCR analysis revealed the presence of TuJ1+ neurons, S100+ glia and Sox10+ stem cells within ENSC neurospheres, as well as expression of key neuronal subtype genes, at levels comparable to SC tissue. Following ENSC transplantation to an ablated region of chick embryo SC, donor neurons were found up to 12 days later. These neurons formed bridging connections within the SC injury zone, aligned along the anterior/posterior axis, and were immunopositive for TuJ1. These data provide early proof of principle support for the use of ENSCs for SCI, and encourage further research into their potential for repair.

Key words

Enteric neural stem cells; cell transplant; spinal cord; chick embryo; enteric nervous system; central nervous system

Introduction

Trauma of the spinal cord results in immediate, life-changing paralysis, affecting around 40,000 individuals in the UK (Gall and Turner-Stokes, 2008). Due to the debilitating nature and high prevalence of spinal cord injury (SCI) a wide variety of therapeutic options have been explored, including the use of stem cells (Assinck et al., 2017; Goulao and Lepore, 2016; Nagoshi and Okano, 2017; Oliveri et al., 2014). Stem cells offer the potential to support endogenous recovery and replace lost neurons in SCI as well as form bridging structures and allow axonal regeneration across the injury site (Bottai et al., 2010; Cusimano et al., 2012; Moreno-Manzano et al., 2009; Salazar et al., 2010). These attributes have been demonstrated using a variety of stem cell sources, but finding a *single* stem cell source that fulfills *all* the above qualities has proven difficult.

Enteric neural stem cells (ENSCs) comprise the renewing cell population within the enteric nervous system (ENS), the intrinsic innervation of the gastrointestinal tract (Burns and Thapar, 2014; Furness, 2012). The ENS is derived in its entirety from vagal and sacral neural crest cells arising from the dorsal neural tube during embryogenesis (Burns and Le Douarin, 1998; Espinosa-Medina et al., 2017; Le Douarin, 1973; Nagy et al., 2012). These precursor cells migrate into and along the gut to form the ENS, giving rise to neurons, glia and self-renewing ENSCs (Kruger et al., 2002; Natarajan et al., 1999; Suarez-Rodriguez and Belkind-Gerson, 2004). ENSCs have been detected in the gut from embryonic stages through to late adulthood, and have been successfully isolated from human patients up to 84 years of age (Metzger et al., 2009a). This finding and especially the fact that ENSCs can be harvested from the gut using minimally invasive techniques such as endoscopy, suggests that such cells could be used for autologous transplantation (Burns and Thapar, 2014; Burns et al., 2016; Metzger et al., 2009b). For this approach, ENSCs would be harvested from the gut of a patient, expanded and perhaps manipulated in culture before transplanting them back into the same patient into other (diseased) gut regions, or regions of the body where neurons are lost or damaged e.g. spinal cord in SCI. Previous studies from our laboratory have demonstrated that transplantation of ENSCs into murine gut resulted in production of appropriate neuroglial cell lineages, with functional cell

integration into endogenous ENS networks (Cooper et al., 2016). When transplanted into a mouse model of gut dysmotility, ENSCs were capable of replacing lost neuronal populations and of restoring gut function (McCann et al., 2017).

Although pre-clinical animal studies of ENSCs have to date focused almost exclusively on ENS repair (Burns et al., 2016; Stamp, 2017) the ENS shares several features with the SC that strongly support the use of ENSCs as a stem cell-based therapy for SCI. Immunofluorescence analysis of cultured murine ENSCs has revealed TuJ1+ neurons, S100+ glia and SOX10+/S100- labelled stem cells (Metzger et al., 2009b; Natarajan et al., 2014), all of which are markers that are also expressed in central nervous system (CNS) tissues (Barnabe-Heider et al., 2010; Beaudet et al., 2015). Thus, there is a rationale for using ENSCs to replace cells lost through SCI. In addition, the ENS and CNS share a common neurotransmitter pool (McConalogue and Furness, 1994; Wade et al., 1994), enabling continual bi-directional communication of the ENS and SC through several nerve tracts (Furness, 2012). This supports the idea that transplanted ENSCs may be able to both differentiate towards SC neuronal subtypes, and respond to SC-derived signaling.

The aim of this study was to test the ability of ENSCs to integrate within the developing spinal cord. We show that previously established chimeric grafting techniques using transgenic GFP chick embryos (Burns et al., 2002; Delalande et al., 2015; Freem et al., 2012) enabled effective fluorescent labelling and isolation of ENSCs and their derivatives. Furthermore, we demonstrate that chick gut-derived ENSCs generated neurospheres containing a heterogeneous mix of neurons, glia, and stem cells, similar to previous reports of murine ENSCs (Natarajan et al., 2014). These neurospheres expressed markers of key SC neuronal subtypes at levels comparable to SC tissue. Using the chick embryo as host, we confirm ENSC survival and integration following transplantation into the injured SC. Transplanted cells differentiated towards a neuronal rather than an astrocytic fate and formed bridging structures across the injury site. These results encourage further investigation into the use of ENSCs for SCI.

Materials and Methods

Labelling of ENSCs

GFP+ ENSCs were generated using previously published techniques (Delalande et al., 2015). Briefly, fertilised wild type (WT, Medeggs, UK) and GFP chicken eggs (The Roslin Transgenic Chicken Facility, Scotland) were incubated for 36 hours to E1.5. The vagal neural tube (NT) of GFP embryos, located between somites 1-7 was isolated and grafted into WT embryos with the corresponding region ablated. Embryos were returned to the incubator and allowed to develop to E14.

FACS (fluorescence activated cell sorting) isolation of GFP+ ENSCs

At E14, chick embryos were sacrificed and the intestinal tract harvested in ice-cold PBS (Mg2+/Ca2+ free, Sigma Aldrich, UK) with penicillin/ streptomycin (P/S, 1%, Sigma Aldrich, UK). Gut tissue was digested in dispase/ collagenase (1mg mL^{-1}, Roche, UK). Cells were sorted based on GFP fluorescence using a MoFlow XDP (Beckman Coulter), re-suspended in neural stem cell media (NSM, DMEM F12 (Sigma Aldrich, UK), N2, B27 (Invitrogen, UK), P/S, FGF and EGF (20ng mL^{-1}, Peprotech, London) and plated onto fibronectin (Sigma Aldrich, UK)-coated plates. The following day media was replaced to remove dead cells, and changed every two days thereafter. If colonies grew confluent they were passaged, by washing in PBS and digested in trypsin for 2 minutes at 37°C. Cells were dissociated, centrifuged and re-plated onto fresh 2% fibronectin-coated dishes (50,000 cells mL^{-1}).

Spinal cord cell culture and viral labelling

Chick SCs were harvested at E14 into ice-cold PBS with P/S and the meninges removed. Following digestion in Trypsin (37°C) SCs were manually dissociated and plated onto fibronectin-coated dishes. Prior to co-culture experiments with GFP-labelled ENSCs, SC-derived cells were labelled with mCherry lentivirus as previously published (Natarajan et al., 2014). Briefly, cells were incubated with 100µL per 10^5 cells (multiplicity of infection 2-5) of a self-inactivating mCherry

lentiviral construct diluted in NSM, for 48 hours to allow efficient transduction and viral inactivation. Following this, media was replaced with fresh NSM.

Co-culture of ENSCs and spinal cord-derived cells

In vitro co-cultures were used to test the potential of ENSC and SC-derived cell interactions. Independently cultured FAC-sorted ENSCs and viral-labelled SC cells were passaged and plated in equal numbers onto fibronectin-coated dishes at a combined density of approximately 50,000 cells mL^{-1}.

Transplantation of ENSC neurospheres into chick embryo spinal cord

A small region of the neural tube was microsurgically ablated, equivalent to the length of 1 somite, at the level of somite 7 in E1.5 WT embryos. We refer to this ablated region as the site of spinal cord injury throughout this study. A single GFP+ ENSC neurosphere was transplanted into the ablated space and the egg returned to the incubator. Transplanted embryos were harvested at timed intervals up to E13.5 and fixed in 4% paraformaldehyde (PFA, Sigma Aldrich, UK).

Cryosectioning and immunofluorescence staining

Gelatin-embedded samples were snap frozen, stored at -80°C until required and sectioned using a Leica CM1900 UV Cryostat (Leica Microsystems, UK) at -22°C. Section thickness was 10-20µm. Slides were stored at -20°C until required. Slides, whole-mount samples or cell cultures were post-fixed in 4% PFA, blocked (0.1% Triton X100 (Sigma Aldrich, UK), 1% bovine serum albumin, 0.15% glycine in 1XPBS) for 1 hour and incubated in primary antibody (Table 1) diluted in blocking solution overnight at 4°C. Secondary antibody (Table 2) was applied in blocking solution for 2 hours (RT) and slides were mounted using Vectashield (hard set with DAPI, Dako, UK) and stored at 4°C.

Quantification of cell spread

To determine the extent of ENSC cell projection/spread from the transplantation site within the developing neural tube, sections of transplanted embryos were stained with an anti-GFP antibody and images collected using an ORCA-R2

cooled CCD camera mounted on an Olympus 1X70 inverted microscope. Total spread along the anterior/posterior axis was captured, and where appropriate, images were collated into a tile scan using MosaicJ on FIJI (Schindelin et al., 2012). For each embryo, the section demonstrating the greatest spread was selected. For each age under examination, n=3 embryos were used.

RNA extraction

Tissue samples were homogenized and immersed in Trizol (Invitrogen, UK). This was incubated with chloroform (RT) and centrifuged at 12,000g for 15 minutes at 4°C. The upper aqueous phase was isolated, mixed with 70% ethanol and transferred to an RNeasy Mini spin column (Qiagen, Germany). The manufacturer's protocol was then followed. For cells, the manufacturer's protocol was followed without modification. RNA yield was quantified using a NanoDrop 1000 (Thermo Scientific, UK).

cDNA synthesis

100ng of RNA was used for each reaction. This was added to 4µL 5X VILO reaction mix and 2µL 10X Superscript Enzyme Mix (Life Technologies, Paisley, UK). The volume was adjusted to 20µL with DEPC-treated water. Synthesis was conducted using a Thermofisher Cycler as per the manufacturer's protocol.

PCR

Primers were designed with amplification product sizes of 100-200bp (Sigma Aldrich, UK?) (Table 3). PCR was used to verify primer accuracy and annealing conditions (Table 4). qRT-PCR samples were assayed (Table 5) in triplicate normalized to the house-keeping gene GAPDH, and analysed using the ABI prism 7500 sequence detection system (ThermoFisher Scientific, Germany) using quantitect SYBR green PCR kit (Qiagen, Germany) according to the manufacturer's instructions.

Statistical analysis

qRT-PCR and cell spread data were analysed by student's t test (two-tailed) or analysis of variance (ANOVA). Survival of transplanted and non-transplanted

groups was compared using the Log-rank (Mantel-Cox) test. GraphPad Prism software was used for all analyses, with p values of <0.05 considered significant.

Results

Chick^{GFP}-chick^{WT} grafting robustly labels the ENS and allows efficient isolation of ENSCs

To facilitate isolation of ENSCs, the neural tube, between somites 1-7, was grafted from GFP chick embryos into WT chick embryos at E1.5 (Fig. 1A). This procedure specifically labelled the neural crest-derived precursor cells of the ENS and their derivatives (neurons, glia, ENSCs) throughout the GI tract (Fig. 1B). At E6.5 GFP+ cells had colonised the GI tract to the level of the caeca (Fig. 1C). Whole mount staining of the GFP-labelled GI tract with the neuronal marker TuJ1 revealed the differentiation wavefront ~3mm behind the migration wavefront of GFP+ cells (Fig. 1C). The nerve of Remak (NOR), adjacent to the intestine, is derived from the sacral neural crest, not the vagal neural crest (the site of grafting), and therefore does not contain GFP+ cells. Serial colonic cryosections from E8 chimeras revealed GFP+ expression within the myenteric and submucosal plexuses. GFP+ immunofluorescence co-localised with both HNK1 (Fig. 1D) and TuJ1 (Fig. 1E), confirming that GFP+ cells are of neural crest origin, and that they had differentiated towards a neuronal lineage, respectively. ENS architecture within the chimeric gut was consistent with previously published descriptions demonstrating that tissue grafting does not cause abnormal development.

Robust GFP+ labelling allowed for specific isolation of GFP+ by FACS. This revealed clear distinction of the labelled GFP+ neural crest-derived cells (green) and negative non-neural crest cells (Fig. 2A). At E14 chimeras were sacrificed and the GI tract distal to the stomach removed and dissociated into single cell suspension. Typically, around 4% of FACS 'events' (cells) from E14 chimeric gut were selected as GFP+. Isolated GFP+ cells were cultured for up to 3 months with no loss in GFP signal. These cultures readily formed neurospheres, which typically became free-floating after approximately 2 weeks. Examination via immunostaining revealed that the GFP+ neurospheres contained numerous

TuJ1+ (Fig. 2B) and HuC/D+ neurons (data not shown), the predominant cell type lost during spinal cord injury.

To assess the ability of ENSC-derived cells to integrate with SC-derived cells, an *in vitro* co-culture assay was performed. Unsorted SC-derived cells were fluorescently labelled with mCherry lentivirus (labeling efficiency 71.2±6.8%, to allow for specific identification of cell types. At 10 days, GFP+ ENSC-derived cells established close associations with mCherry+ SC-derived cells, including co-extension of axons alongside SC-derived cells (Fig. 2C, arrowhead) and cellular contacts between ENSC-derived cells and SC-derived cells (Fig. 2C, arrow). When co-cultures were left for extended periods (between 2-4 weeks in culture) the formation of mixed-population neurospheres was observed (Fig. 2D). These results suggest that the formation of functional interconnections between the two cell populations is possible but further studies will need to be performed in order to confirm this.

ENSCs express stem cell and neuronal subtype markers at comparable levels to SC tissue

The close association of cellular processes observed in co-culture experiments suggested the potential of ENSC- and SC-derived cell communication. However, the relative expressions of neurotransmitters of ENS-derived cultures and CNS tissues have not been compared previously. To this end, we used qRT-PCR analysis to compare gene expression between independently cultured enteric neurospheres and non-cultured SC-tissue (harvested at E14). To determine the effect of cell culture on gene expression, RNA extracted from uncultured gut (E14) was used as a control.

A comparison of gene expression levels of the major cell types typically found within neurospheres revealed expression of TuJ1 (neurons), S100 (glia), SOX10 (progenitor/stem cells), and p75 (neural crest cells), in both gut and SC tissue (relative to GAPDH expression). S100 and SOX10 expression was significantly higher in SC tissue compared to gut tissue (0.055 *vs* 0.040, p=0.0098, and 0.100 *vs* 0.045, p=0.0049, respectively). TuJ1 was strongly expressed in both tissues, although significantly higher in SC-derived tissue (0.230 *vs* 0.059, p=0.0006, Fig. 3A). An analysis of gene expression in ENSC

neurospheres revealed similar levels of all markers under examination to uncultured gut tissue, implying that the culture of ENSC neurospheres did not adversely affect gene expression. A comparison of SC and cultured ENSC-derived cell expression levels appeared similar to that between SC and gut tissue. The relative expression of TuJ1 was significantly higher in SC tissue than in ENSC neurosphere cultures (0.236 *vs* 0.058, p= 0.049, Fig. 3B), and levels of S100 were again slightly higher in SC tissue compared to ENSC cultures. However, compared to the relative expression of SOX10 in uncultured gut, levels within ENSC neurospheres were increased (0.045 *vs* 0.225, p=0.0753, n=3). SOX10 expression of ENSC cultures was also higher than expression in SC tissue.

Next, we sought to determine the expression of key neuronal subtypes present within the ENSC cultures, gut and SC tissue. We analysed the relative expression levels of five neurotransmitters, selected based on their particular relevance to spinal cord injury (Gwak et al., 2006; Hamada et al., 1996; Kapitza et al., 2012; Murray et al., 2010; Panter et al., 1990). All subtype genes under examination - nNOS (NO), TPH1 (serotonin), GLS1 (glutamine), ChAT (acetylcholine) and GAD (GABA) were expressed in both gut and SC tissue. nNOS, TPH1, GLS1 and ChAT expression levels were similar in gut and SC tissue. The relative expression of GAD (GABA) was significantly higher in SC than gut tissue (0.118 *vs* 0.026, p=0.0309, Fig. 3C). In both populations, acetylcholine expression was highest. qRT-PCR analysis of ENSC cultures appeared broadly similar to whole-gut expression, although the expression levels of all neuronal subtype genes appeared to decrease with time in culture (expression levels of nNOS and TPH1 were slightly, but significantly lower in ENSC cultures compared to whole SC tissue, 0.040 *vs* 0.060, p= 0.0021, and 0.025 *vs* 0.037, p=0.0054), with the exception of acetylcholine (Fig. 3D). Thus, these experiments demonstrated that cultured enteric neurospheres express neuronal subtype markers at levels similar to SC tissue.

Transplanted ENSCs integrate and form bridging structures within the injured spinal cord

The propensity of ENSC- and SC-derived cells to interact *in vitro*, combined with the expression of common cell and neuronal subtypes within both populations

demonstrated the potential for ENSC-derived cells to integrate with endogenous cells in the spinal cord environment, and to potentially replace cells lost during an injury. To test this further *in vivo*, GFP+ ENSC-derived neurospheres were transplanted into the developing chick neural tube at E1.5. In order to perform the neurosphere transplants, a small region of the neural tube, one somite in length, was microsurgically ablated. This ablated part of the neural tube, the region into which neurospheres were transplanted, is subsequently referred to as the site of spinal cord injury (Fig.1). Following transplant, embryos were harvested at E5.5, E7.5, E9.5 and E13.5 to assess cell survival, spread and differentiation. There was no difference in survival between transplanted and non-transplanted control groups (log-rank Mantel-Cox test, p=0.5607).

GFP+ cells were present within the SC 4 days post-transplant at E5.5, with GFP expression strong enough to allow visualisation of both cell bodies and processes. Upon stereoscopic examination, GFP+ cells had spread from the transplantation site within the cervical spinal cord, as expected following transplantation, into the vagal neural tube. The majority of migrating cell streams aligned in an anterior-posterior (A/P) direction (Fig. 4A,B). Transverse sections showed that GFP+ transplanted ENSCs were almost exclusively localised to the white matter (WM), as indicated by intense TuJ1+ staining (Fig. 4D), and surrounded the entire SC. Longitudinal cryosections of the spinal column revealed dense clusters of GFP+ cells around the injured region of the developing spinal cord. These cells appeared to form bridging connections across the injury zone and could be seen within spinal cord tissue both anterior and posterior to the injury site (Fig. 4E). Some spread into dorsal root ganglia was also observed. Spread of GFP+ cells was almost exclusively confined to TuJ1+ structures, with only a few cells found in non-neuronal regions dorsal to the spinal cord. Careful examination of the intestines of transplanted animals revealed no GFP+ cells in this organ (data not shown).

By E7.5 stereoscopic examination showed a more obvious alignment of transplanted GFP+ cells along the A/P axis, with considerably greater overall spread (Fig. 5A,B). Similar to E5.5 embryos, transverse sections of transplanted embryos harvested at E7.5 revealed localisation to the white matter. However, transplanted cells appeared concentrated towards the dorsal spinal cord, with

less cells found more ventrally (Fig. 5C). At E7.5, spread of GFP+ transplanted cells to surrounding tissues, neuronal or otherwise, was less evident. Longitudinal sections again showed GFP+ cells spreading across the injury zone, both extending into the ablated region and localised to the anterior and posterior spinal cord tissue (Fig. 5D, arrow). Consistent with transverse sections, most cells were observed towards the dorsal aspect of the cord.

By E9.5 the thickness of overlying structures dorsal to the SC made stereoscopic examination of GFP+ cell spread technically not feasible. However, transverse cryosections revealed similar localisation patterns to earlier ages, with more cells moving into the grey/white matter border and isolated cells within the grey matter itself (Fig. 6A). Continuing the trend observed between E5.5 and E7.5 transplanted embryos, transplanted cells were now almost exclusively localised to the dorsal spinal cord. Longitudinal cryosections revealed multiple GFP+ ENSCs within the injury zone, with the vast majority of cells localised to remaining TuJ1+ structures (Fig. 6B).

At E13.5, the latest time point examined, GFP+ transplanted cells had formed substantial bridges across the injury zone and continued spreading through the white matter of the spinal cord (Fig. 7A, D). Transverse sections revealed that distal to the injury, transplanted cells localised to the white matter (Fig. 7B), whereas at the injury zone GFP+ cells did not appear to show any such preference. The predominantly dorsal localisation observed at E7.5 and E9.5 was not observed at E13.5.

Having demonstrated the integration of ENSCs with SC cells in co-culture experiments, and successfully shown similar integration of transplanted cells into the SC after injury *in vivo*, we next examined the fate of transplanted ENSCs. An examination of transplanted GFP+ cells revealed numerous cell bodies aligned along the A/P axis, both within the injury zone and spared spinal cord tissue. The extent of cell spread along the A/P axis increased with time post transplantation, and this trend was confirmed with quantification across the four stages analysed (Supp. Fig. 1A). A statistically significant difference in the mean spread across all groups was also found using ANOVA ($F(3,8)=13.9$, $p=0.002$), with significantly greater spread observed in transplants harvested at E9.5 (3206.2μm, $p=0.0077$) and E13.5 (7373.2μm, $p=0.0127$) compared to E5.5

(1101.7μm, Supp. Fig. 8A). Additionally, we found no transplanted cells that co-expressed GFAP at E13.5, the latest time point examined (Supp. Fig. 1B). Contrastingly, immunostaining revealed that many donor cells were TuJ1+ (Supp. Fig. 1C).

Discussion

The chick embryo has previously been demonstrated to accurately recapitulate human SCI pathology (Ferretti and Whalley, 2008; Ferretti et al., 2003). We thus took advantage of this animal model to both robustly label and selectively isolate vagal neural crest-derived ENS cells (neurons, glia and enteric neural stem cells), and to test the ability of ENSCs to integrate within the early spinal cord.

As an initial step to test the potential of cells derived from the ENS to integrate within the CNS, ENSCs were co-cultured with SC-derived cells. Results showed that the two populations had a propensity to interact, demonstrated by ENSC and SC-derived axons extending alongside and towards one another. These observations supported the idea that enteric-derived cells could integrate within the spinal cord following *in vivo* transplantation, and potentially serve as bridges to encourage endogenous axon growth. Previous studies, where stem cell transplantations induced partial functional recovery, identified the establishment of lesion-spanning bridges that endogenous axons could cross as important for motor/sensory improvement (Assinck et al., 2017; Popovich, 2012). Further support for the idea that enteric neural cells could integrate into the spinal cord came from qRT-PCR analysis, which revealed common expression of neurotransmitters examined in both gut and SC tissue. Together, these findings suggest that enteric neural cells are similar in their expression of key neuronal subtype markers, and that ENS and SC-derived cells are likely capable of functional integration. This data allowed us to move to an *in vivo* model whereby ENSCs were transplanted into the spinal cord.

Following transplant, the vast majority of GFP+ ENSCs localised within the spinal cord and dorsal root ganglia. Occasional cells found outside TuJ1+ neural tissues were restricted to tissues dorsal to the spinal cord, and likely reflect transplantation artifacts following ectoderm closure over the neural tube (whereby some GFP+ cells may have been enclosed). In support of this

conclusion, GFP+ transplanted cells were not found in TuJ1-negative tissue ventral to the spinal cord. It is unlikely that small numbers of cells in these ectopic locations would affect therapeutic application of ENSCs, as treatment would involve direct transplantation into the adult injury site when no such developmental morphogenic processes occur.

At all ages examined, transplanted GFP+ ENSCs localised to the future white matter (myelin does not form until around E13 (Macklin and Weill, 1985)), and only rarely were they found in the grey matter. Previous studies investigating transplantation of alternative sources of stem cells into the embryonic chick neural tube have shown relatively poor localisation properties. Following transplantation of rat amniotic fluid stem cells (AFSCs) into the injury site at E2.5, Prasongchean *et al* found donor cells mostly in the central canal or near the dorsal root ganglia, with no apparent integration (Prasongchean et al., 2012). In contrast, the results of ENSC transplantation described here are more consistent with observations by *et al*., who used the chick embryo as a model organism to assess differentiation following transplantation of induced pluripotent cell-derived motoneurons (iPSCMNs) into the developing neural tube (Toma et al., 2015). Their study revealed that transplanted iPSCMNs localised to spinal cord white matter, with projections extending into the PNS, similar to the results presented here. Such localisation was also observed by Belkind-Gerson *et al* (Belkind-Gerson et al., 2016). These authors demonstrated that tail vein delivery of ENSCs into mice resulted in homing of ENSC-derived cells to an injury site and white matter within the brain. Despite systemic delivery, ENSC-derived cells were absent in other neural crest-derived tissues, including the intestines, suggesting injury as a cell localisation cue.

A key finding of this study is that following transplantation ENSCs formed connecting structures across the injury zone. Here, ENSCs were usually found within residual TuJ1+ structures, and occasionally in TuJ1- regions, demonstrating their potential to bridge the anterior and posterior SC. In addition, transplanted cells within the SC often aligned along the A/P axis. Correct alignment is an objective of many stem cell transplantation therapies. The common alignment along the anterior-posterior axis of transplanted ENSCs

is thus a significant finding, and strongly supports the potential of ENSCs to form bridges for endogenous regeneration in SCI.

We also found that the spread of cells along the A/P axis increased significantly with time post-transplant. While it is plausible that this spread was due to growth of the developing tissue, it is likely that at least to a certain degree, this represents an active process of transplanted cells. Firstly, axonal projection was included in these measurements, known to be an active process involving extension of the growth cone and response to attractive/repellent stimuli (Lowery and Van Vactor, 2009). Secondly, for the anterior-posterior increase in spread to be entirely related to growth a similar extension along the left-right axis of the embryo would have been expected. If anything, we noticed a decrease in the extent of transplanted cell spread into the surrounding PNS. While this spread was less than that observed following injection of dissociated cells into the lumen (Prasongchean et al., 2012; Zhao et al., 2013) it is likely more reflective of the extent of cell spread that would be desired following transplantation into adult human spinal cord, in which transplantation would similarly require extension of axons/cells across the injury site, rather than extensive migration through the lumen. A number of studies demonstrated predominant lesion-localisation of transplanted cells, allowing endogenous axons to extend into, but not past, the injury zone (Bonner et al., 2011; Fawcett, 2008; Lu et al., 2003; Lu et al., 2012). The data presented here, showing the ability of transplanted cells to survive in tissue both anterior and posterior to the injury zone, demonstrates the ability of transplanted ENSCs to integrate more fully, providing bridges into and across the injury site, similar to findings by Lu *et al* (Lu et al., 2012).

The types of cells that form and comprise a bridging structure are likely to be highly important. Indeed, neuronal differentiation has often been cited as the causal factor behind functional recovery in SCI following stem cell transplantation (Abematsu et al., 2010; Lu et al., 2012). However, this has proved difficult to achieve, with many publications reporting mostly glial differentiation following transplantation of pluripotent (Cao et al., 2001) or neural stem cells (Shihabuddin et al., 2000; Vroemen et al., 2003), a potentially problematic finding considering that any glia produced may contribute to the glial scar.

Neuronal differentiation of an autologous, easily accessible stem cell source has proved similarly challenging. For example, MSC differentiation towards a neuronal phenotype has proven inconsistent even *in vitro* (Scuteri et al., 2011), and *in vivo* differentiation has been questioned (Parr et al., 2008; Qu and Zhang, 2017). Some have even suggested that astrocytic differentiation of transplanted stem cells may be the default pathway (Kang et al., 2012; Nakamura and Okano, 2013). In contrast, we found frequent examples of transplanted neurons, and no evidence of ENSC differentiation towards an astrocytic lineage following transplantation. It should be noted that in the current study, a heterogenous population of neurons and stem cells was transplanted. Previous characterization of neurospheres within our laboratory has revealed the presence of both immature and mature neuronal markers (Binder et al., 2015; Cooper et al., 2016; McCann et al., 2017; Metzger et al., 2009b). These findings are further supported by the qRT-PCR data in this current paper demonstrating expression of markers involved in synthesis of a variety of neurotransmitters. Future work will be aimed at examining the extent to which transplanted ENSCs contribute to the donor neural population in the host spinal cord post-transplant, including specific neural subtypes. Notably, Belkind-Gerson *et al* reported neuronal differentiation of ENSCs following transplantation into the brain (Belkind-Gerson et al., 2016) and previous studies within our lab showed neurogenesis following ENSC transplant into the gut using labelling with BrdU (Cooper et al., 2016; McCann et al., 2017), making ENSCs a promising source of replacement neurons following SCI.

The work described in this paper demonstrates for the first time that ENSCs can form bridging connections across a SC injury zone and potentially repopulate the injury cavity. Transplanted ENSCs survived, differentiated into neurons and extended axonal processes through the spinal cord. Further, transplanted ENSC cell-spread along the anterior posterior axis increased with time post-transplant. Supporting *in vitro* work demonstrated that ENSCs form common neuronal subtypes with the SC, suggesting their potential to form functional bridges through the injury zone following transplantation. Future studies will progress this data towards adult models of SCI, and will be aimed at

providing further evidence that ENSCs can serve as a viable source of stem cells for SCI.

Acknowledgements

The authors would like to thank Dr Ayad Eddaoudi, Ms Stephanie Canning (UCL Great Ormond Street Institute of Child Health Flow Cytometry Facility) and Dr Dale Moulding (UCL Great Ormond Street Institute of Child Health Imaging Facility) for technical assistance. Research conducted at UCL Great Ormond Street Institute of Child Health is supported by the NIHR Great Ormond Street Hospital Biomedical Research Centre. The views expressed in this manuscript are those of the author(s) and not necessarily those of the NHS, the NIHR or the Department of Health. This work was funded by a grant from the Anatomical Society awarded to AJB.

Author Contributions

AJB and NT conceived the project, acquired funding and together with BJ and CJM designed experiments. BJ, CJM and AJB acquired data and all authors interpreted data. All authors drafted and critically revised the manuscript.

References

Abematsu, M., Tsujimura, K., Yamano, M., Saito, M., Kohno, K., Kohyama, J., Namihira, M., Komiya, S., and Nakashima, K. (2010). Neurons derived from transplanted neural stem cells restore disrupted neuronal circuitry in a mouse model of spinal cord injury. J Clin Invest *120*, 3255-3266.

Assinck, P., Duncan, G.J., Hilton, B.J., Plemel, J.R., and Tetzlaff, W. (2017). Cell transplantation therapy for spinal cord injury. Nat Neurosci *20*, 637-647.

Barnabe-Heider, F., Goritz, C., Sabelstrom, H., Takebayashi, H., Pfrieger, F.W., Meletis, K., and Frisen, J. (2010). Origin of new glial cells in intact and injured adult spinal cord. Cell Stem Cell *7*, 470-482.

Beaudet, M.J., Yang, Q., Cadau, S., Blais, M., Bellenfant, S., Gros-Louis, F., and Berthod, F. (2015). High yield extraction of pure spinal motor neurons, astrocytes and microglia from single embryo and adult mouse spinal cord. Sci Rep *5*, 16763.

Belkind-Gerson, J., Hotta, R., Whalen, M., Nayyar, N., Nagy, N., Cheng, L., Zuckerman, A., Goldstein, A.M., and Dietrich, J. (2016). Engraftment of enteric neural progenitor cells into the injured adult brain. BMC Neurosci *17*, 5.

Binder, E., Natarajan, D., Cooper, J., Kronfli, R., Cananzi, M., Delalande, J.M., McCann, C., Burns, A.J., and Thapar, N. (2015). Enteric neurospheres are not specific to neural crest cultures: implications for neural stem cell therapies. PLoS One *10*, e0119467.

Bonner, J.F., Connors, T.M., Silverman, W.F., Kowalski, D.P., Lemay, M.A., and Fischer, I. (2011). Grafted neural progenitors integrate and restore synaptic connectivity across the injured spinal cord. J Neurosci *31*, 4675-4686.

Bottai, D., Cigognini, D., Madaschi, L., Adami, R., Nicora, E., Menarini, M., Di Giulio, A.M., and Gorio, A. (2010). Embryonic stem cells promote motor recovery and affect inflammatory cell infiltration in spinal cord injured mice. Experimental Neurology *223*, 452-463.

Burns, A., and Thapar, N. (2014). Neural stem cell therapies for enteric nervous system disorders. Nat Rev Gastroenterol Hepatol *11*, 317-328.

Burns, A.J., Delalande, J.M., and Le Douarin, N.M. (2002). In ovo transplantation of enteric nervous system precursors from vagal to sacral neural crest results in extensive hindgut colonisation. Development *129*, 2785-2796.

Burns, A.J., Goldstein, A.M., Newgreen, D.F., Stamp, L., Schafer, K.H., Metzger, M., Hotta, R., Young, H.M., Andrews, P.W., Thapar, N., *et al.* (2016). White paper on guidelines concerning enteric nervous system stem cell therapy for enteric neuropathies. Dev Biol *417*, 229-251.

Burns, A.J., and Le Douarin, N.M. (1998). The sacral neural crest contributes neurons and glia to the post-umbilical gut: spatiotemporal analysis of the development of the enteric nervous system. Development *125*, 4335-4347.

Cao, Q.L., Zhang, Y.P., Howard, R.M., Walters, W.M., Tsoulfas, P., and Whittemore, S.R. (2001). Pluripotent stem cells engrafted into the normal or lesioned adult rat spinal cord are restricted to a glial lineage. Exp Neurol *167*, 48-58.

Cooper, J.E., McCann, C.J., Natarajan, D., Choudhury, S., Boesmans, W., Delalande, J.M., Vanden Berghe, P., Burns, A.J., and Thapar, N. (2016). In Vivo Transplantation of Enteric Neural Crest Cells into Mouse Gut; Engraftment, Functional Integration and Long-Term Safety. PLoS One *11*, e0147989.

Cusimano, M., Biziato, D., Brambilla, E., Donega, M., Alfaro-Cervello, C., Snider, S., Salani, G., Pucci, F., Comi, G., Garcia-Verdugo, J.M., *et al.* (2012). Transplanted neural stem/precursor cells instruct phagocytes and reduce secondary tissue damage in the injured spinal cord. Brain *135*, 447-460.

Delalande, J.M., Thapar, N., and Burns, A.J. (2015). Dual labeling of neural crest cells and blood vessels within chicken embryos using Chick(GFP) neural tube grafting and carbocyanine dye DiI injection. J Vis Exp, e52514.

Espinosa-Medina, I., Jevans, B., Boismoreau, F., Chettouh, Z., Enomoto, H., Muller, T., Birchmeier, C., Burns, A.J., and Brunet, J.F. (2017). Dual origin of enteric neurons in vagal Schwann cell precursors and the sympathetic neural crest. Proc Natl Acad Sci U S A *114*, 11980-11985.

Fawcett, J.W. (2008). Bridging spinal cord injuries. J Biol *7*, 25.

Ferretti, P., and Whalley, K. (2008). Successful neural regeneration in amniotes: the developing chick spinal cord. Cell Mol Life Sci *65*, 45-53.

Ferretti, P., Zhang, F., and O'Neill, P. (2003). Changes in spinal cord regenerative ability through phylogenesis and development: lessons to be learnt. Dev Dyn *226*, 245-256.

Freem, L.J., Delalande, J.M., Campbell, A.M., Thapar, N., and Burns, A.J. (2012). Lack of organ specific commitment of vagal neural crest cell derivatives as shown by back-transplantation of GFP chicken tissues. Int J Dev Biol *56*, 245-254.

Furness, J.B. (2012). The enteric nervous system and neurogastroenterology. Nat Rev Gastroenterol Hepatol *9*, 286-294.

Gall, A., and Turner-Stokes, L. (2008). Chronic spinal cord injury: management of patients in acute hospital settings. Clin Med *8*, 70–74.

Goulao, M., and Lepore, A.C. (2016). iPS cell transplantation for traumatic spinal cord injury. Curr Stem Cell Res Ther *11*, 321-328.

Gwak, Y.S., Tan, H.Y., Nam, T.S., Paik, K.S., Hulsebosch, C.E., and Leem, J.W. (2006). Activation of spinal GABA receptors attenuates chronic central neuropathic pain after spinal cord injury. J Neurotrauma *23*, 1111-1124.

Hamada, Y., Ikata, T., Katoh, S., Tsuchiya, K., Niwa, M., Tsutsumishita, Y., and Fukuzawa, K. (1996). Roles of nitric oxide in compression injury of rat spinal cord. Free Radic Biol Med *20*, 1-9.

Kang, E.S., Ha, K.Y., and Kim, Y.H. (2012). Fate of transplanted bone marrow derived mesenchymal stem cells following spinal cord injury in rats by transplantation routes. J Korean Med Sci *27*, 586-593.

Kapitza, S., Zorner, B., Weinmann, O., Bolliger, M., Filli, L., Dietz, V., and Schwab, M.E. (2012). Tail spasms in rat spinal cord injury: changes in interneuronal connectivity. Exp Neurol *236*, 179-189.

Kruger, G., Mosher, J., Bixby, S., Joseph, N., Iwashita, T., and Morrison, S. (2002). Neural Crest Stem Cells Persist in the Adult Gut but Undergo Changes in Self-Renewal, Neuronal Subtype Potential, and Factor Responsiveness. Neuron *35*, 657-669.

Le Douarin, N. (1973). A biological cell labeling technique and its use in expermental embryology. Dev Biol *30*, 217-222.
Lowery, L.A., and Van Vactor, D. (2009). The trip of the tip: understanding the growth cone machinery. Nat Rev Mol Cell Biol *10*, 332-343.
Lu, P., Jones, L.L., Snyder, E.Y., and Tuszynski, M.H. (2003). Neural stem cells constitutively secrete neurotrophic factors and promote extensive host axonal growth after spinal cord injury. Exp Neurol *181*, 115-129.
Lu, P., Wang, Y., Graham, L., McHale, K., Gao, M., Wu, D., Brock, J., Blesch, A., Rosenzweig, E.S., Havton, L.A.*, et al.* (2012). Long-distance growth and connectivity of neural stem cells after severe spinal cord injury. Cell *150*, 1264-1273.
Macklin, W.B., and Weill, C.L. (1985). Appearance of myelin proteins during development in the chick central nervous system. Dev Neurosci *7*, 170-178.
McCann, C.J., Cooper, J.E., Natarajan, D., Jevans, B., Burnett, L.E., Burns, A.J., and Thapar, N. (2017). Transplantation of enteric nervous system stem cells rescues nitric oxide synthase deficient mouse colon. Nat Commun *8*, 15937.
McConalogue, K., and Furness, J.B. (1994). Gastrointestinal neurotransmitters. Baillieres Clin Endocrinol Metab *8*, 51-76.
Metzger, M., Bareiss, P.M., Danker, T., Wagner, S., Hennenlotter, J., Guenther, E., Obermayr, F., Stenzl, A., Koenigsrainer, A., Skutella, T.*, et al.* (2009a). Expansion and differentiation of neural progenitors derived from the human adult enteric nervous system. Gastroenterology *137*, 2063-2073 e2064.
Metzger, M., Caldwell, C., Barlow, A.J., Burns, A.J., and Thapar, N. (2009b). Enteric nervous system stem cells derived from human gut mucosa for the treatment of aganglionic gut disorders. Gastroenterology *136*, 2214-2225 e2211-2213.
Moreno-Manzano, V., Rodríguez-Jiménez, F.J., García-Roselló, M., Laínez, S.,, Erceg, S., Calvo, M. T.,, Ronaghi, M., Lloret, M., Planells-Cases, R., Sánchez-Puelles, J.M., and Stojkovic, M. (2009). Activated Spinal Cord Ependymal Stem Cells Rescue Neurological Function. STEM CELLS *27*, 733–743.
Murray, K.C., Nakae, A., Stephens, M.J., Rank, M., D'Amico, J., Harvey, P.J., Li, X., Harris, R.L., Ballou, E.W., Anelli, R.*, et al.* (2010). Recovery of motoneuron and locomotor function after spinal cord injury depends on constitutive activity in 5-HT2C receptors. Nat Med *16*, 694-700.
Nagoshi, N., and Okano, H. (2017). Applications of induced pluripotent stem cell technologies in spinal cord injury. J Neurochem *141*, 848-860.
Nagy, N., Burns, A.J., and Goldstein, A.M. (2012). Immunophenotypic characterization of enteric neural crest cells in the developing avian colorectum. Dev Dyn *241*, 842-851.
Nakamura, M., and Okano, H. (2013). Cell transplantation therapies for spinal cord injury focusing on induced pluripotent stem cells. Cell Res *23*, 70-80.
Natarajan, D., Cooper, J., Choudhury, S., Delalande, J.M., McCann, C., Howe, S.J., Thapar, N., and Burns, A.J. (2014). Lentiviral labeling of mouse and human enteric nervous system stem cells for regenerative medicine studies. Neurogastroenterol Motil *26*, 1513-1518.

Natarajan, D., Grigoriou, M., Marcos-Gutierrez, C., Atkins, C., and Pachnis, V. (1999). Multipotential progenitors of the mammalian enteric nervous system capable of colonising aganglionic bowel in organ culture. Development *126*, 157-168.

Oliveri, R.S., Bello, S., and Biering-Sorensen, F. (2014). Mesenchymal stem cells improve locomotor recovery in traumatic spinal cord injury: systematic review with meta-analyses of rat models. Neurobiol Dis *62*, 338-353.

Panter, S.S., Yum, S.W., and Faden, A.I. (1990). Alteration in extracellular amino acids after traumatic spinal cord injury. Ann Neurol *27*, 96-99.

Parr, A.M., Kulbatski, I., Wang, X.H., Keating, A., and Tator, C.H. (2008). Fate of transplanted adult neural stem/progenitor cells and bone marrow-derived mesenchymal stromal cells in the injured adult rat spinal cord and impact on functional recovery. Surg Neurol *70*, 600-607; discussion 607.

Popovich, P.G. (2012). Building bridges for spinal cord repair. Cell *150*, 1105-1106.

Prasongchean, W., Bagni, M., Calzarossa, C., De Coppi, P., and Ferretti, P. (2012). Amniotic fluid stem cells increase embryo survival following injury. Stem Cells Dev *21*, 675-688.

Qu, J., and Zhang, H. (2017). Roles of Mesenchymal Stem Cells in Spinal Cord Injury. Stem Cells International *2017*.

Salazar, D.L., Uchida, N., Hamers, F.P., Cummings, B.J., and Anderson, A.J. (2010). Human neural stem cells differentiate and promote locomotor recovery in an early chronic spinal cord injury NOD-scid mouse model. PLoS One *5*, e12272.

Schindelin, J., Arganda-Carreras, I., Frise, E., Kaynig, V., Longair, M., Pietzsch, T., Preibisch, S., Rueden, C., Saalfeld, S., Schmid, B.*, et al.* (2012). Fiji: an open-source platform for biological-image analysis. Nature methods *9*, 676-682.

Scuteri, A., Miloso, M., Foudah, D., Orciani, M., Cavaletti, G., and Tredici, G. (2011). Mesenchymal stem cells neuronal differentiation ability: a real perspective for nervous system repair? Curr Stem Cell Res Ther *6*, 82-92.

Shihabuddin, L.S., Horner, P.J., Ray, J., and Gage, F.H. (2000). Adult spinal cord stem cells generate neurons after transplantation in the adult dentate gyrus. J Neurosci *20*, 8727-8735.

Stamp, L.A. (2017). Cell therapy for GI motility disorders: comparison of cell sources and proposed steps for treating Hirschsprung disease. Am J Physiol Gastrointest Liver Physiol *312*, G348-G354.

Suarez-Rodriguez, R., and Belkind-Gerson, J. (2004). Cultured nestin-positive cells from postnatal mouse small bowel differentiate ex vivo into neurons, glia, and smooth muscle. Stem Cells *22*, 1373-1385.

Toma, J.S., Shettar, B.C., Chipman, P.H., Pinto, D.M., Borowska, J.P., Ichida, J.K., Fawcett, J.P., Zhang, Y., Eggan, K., and Rafuse, V.F. (2015). Motoneurons derived from induced pluripotent stem cells develop mature phenotypes typical of endogenous spinal motoneurons. J Neurosci *35*, 1291-1306.

Vroemen, M., Aigner, L., Winkler, J., and Weidner, N. (2003). Adult neural progenitor cell grafts survive after acute spinal cord injury and integrate along axonal pathways. Eur J Neurosci *18*, 743-751.

Wade, P.R., Tamir, H., Kirchgessner, A.L., and Gershon, M.D. (1994). Analysis of the role of 5-HT in the enteric nervous system using anti-idiotopic antibodies to 5-HT receptors. Am J Physiol *266*, G403-416.

Zhao, J., Sun, W., Cho, H.M., Ouyang, H., Li, W., Lin, Y., Do, J., Zhang, L., Ding, S., Liu, Y.*, et al.* (2013). Integration and long distance axonal regeneration in the central nervous system from transplanted primitive neural stem cells. J Biol Chem *288*, 164-168.

Table 1: Primary antibodies

Antibody	Species	Manufacturer	Concentration
TuJ1	Mouse	Covance	1:500
GFAP	Rabbit	DAKO	1:500
HNK-1	Mouse	Supernatant	1:20
GFP	Rabbit	Invitrogen	1:500

Table 2: Secondary antibodies

Antibody	Species	Manufacturer	Concentration	Absorbance
Anti mouse	Goat	Alexa Fluor	1:500	568
Anti rabbit	Goat	Alexa Fluor	1:500	488
Anti-rabbit	Goat	Alexa Fluor	1:500	568
DAPI	N/A	Sigma Aldrich	1:1000	350

Table 3: Primers used for PCR

Probe target	Primer sequence	Product size	Tm
TuJ1	F: GCCCCGACAACTTCATTTT R: GCAGTCGCAGTTCTCACACT	138	63.8 63.4
p75	F: AGGTGATGGTGAAGGAGTGC R: GACGGTGGTGACAATGTCTG	183	64.2 64.3
S100	F: AGTACTCCGGGAAGGAAGGA R: GTCCAGTGCCTCCATGACTT	144	63.8 64.2
Sox10	F: AGCCTTCACAGGGTTTGCT R: GAGAGGCAGTGGTGGTCTTC	135	63.8 63.9
ChAT	F: AATGCCAGAACCAGAGCACA R: TCAGTCGTCAGCAAGCCAAT	189	65.8 66.0
GAD	F: GACATCCACCGCTAACACCA R: CGCCATCTTTATTCGACCATCC	131	66.0 68.3
GLS1	F: CTTACTCAAGCTTTCAGGAGGAA	194	62.6

	R: TGCCCATCCACTGTGCAAA		69.0
nNOS	F: ATGCTCAACTACCGCCTCAC	117	64.2
	R: AATGGCCCTCTTCTTGGTGG		67.3
TPH1	F: GTGCTGATGTACGGGTCTGA	112	69.3
	R: AGTTCATAGCCAGGTCTGCA		62.5
TPH2	F: CTCTATCCCACCCACGCTTG	159	66.7
	R: AACCGGTCTCACTGTGAAGC		64.3

Table 4: PCR cycling programme

Step	**Temp °C**	**Time**
1	94	3 minutes
2	94	30 seconds
3	60	1 minute
4; go to step 2, 35 cycles	72	30 seconds
5	72	2 minutes
6	4	Hold

Table 5: qRT-PCR cycling programme

Step	**Temp °C**	**Time**
1	95	15 min
2	95	20 seconds
3	60	30 seconds
4; go to step 2, 40 cycles	72	30 seconds

Figure Legends

Figure 1. GFP chick intraspecies grafting efficiently labels the enteric nervous system of the gastrointestinal tract.

(A) Schematic representing chick embryo tissue grafting methodology. Neural tubes from the vagal region (adjacent to somites 1-7) of GFP+ E1.5 embryos were isolated and grafted into WT hosts in which the corresponding neural tube region was microsurgically ablated. Embryos developed for a further 12.5 days, at which point the intestines were harvested, stripped of mesentery, and dissociated into single cell suspension. GFP+ cells were isolated by FACS and expanded in culture to form GFP+ neurospheres for transplantation into E1.5 embryos. (B) Vagal neural tube grafting specifically labeled neural crest-derived tissues including the ENS of the GI tract. (C) At E6.5, GFP+ cells were observed along the gut, extending caudal to the caeca into the colon (C, arrow and C'). Following the migration wavefront TuJ1+/GFP+ cells were present (C, arrowhead and C''). (D, E) At E8.5, the GI tract was completely colonized by migrating neural crest cells. Transverse sections of the colon revealed the formation of GFP+ myenteric and submucosal plexuses. GFP+ cells co-expressed the neural crest cell marker HNK-1 (D'') and the neuronal marker TuJ1 (E''). NOR - nerve of Remak. Scale bars: C = 500μm; D,E = 250μm.

Figure 2. GFP+ enteric neural crest-derived cells form neurospheres and interconnections with CNS-derived cells *in vitro*.

After GFP tissue grafting, embryos were harvested at E14 and the gastrointestinal tract removed. (A) Gut tissues were dissociated into single cell suspension and sorted based on GFP expression and size. GFP negative populations were collected and cultured as controls. (B) Following FACS isolation, GFP+ graft-derived cells formed free-floating neurospheres after 1-2 weeks in culture. The majority of cells within neurospheres were immunopositive for the neuronal marker TuJ1 (B'). (C) GFP+ neural crest-derived cells were co-cultured with spinal cord (SC)-derived cells (labeled with an mCherry lentiviral construct). C' and C'' show higher magnification selections of C. (D) After several days in culture SC-derived cells (red, D') and ENS-derived

GFP+ cells (D'') aggregated to form mixed-population neurospheres. Scale bars: B,C = 50μm; D = 100μm.

Figure 3. Cultured enteric neural crest-derived cells and whole SC samples express common neuroglial markers.

(A) Uncultured gut and SC tissues were analysed by qRT-PCR to determine relative expression levels of the neurosphere markers. TuJ1 (pan neuronal marker), S100 (glia), Sox10 (progenitor/stem cells) and the neural crest marker p75. (B) Expression levels of the neurosphere markers were assessed in cultured ENS-derived neurospheres and compared with expression in the SC. (C) Expression levels of specific neuronal subtypes were compared between uncultured gut and SC samples, including nNOS (NO), TPH1 (serotonin), GLS1 (glutamine) and ChAT (acetylcholine) and GAD (GABA) (D). The expression levels of these neuronal subtype markers were compared between ENS-derived neurosphere cultures and uncultured SC samples. nNOS, TPH1, GLS1, GAD n=3, ChAT n=2. * - p=<0.05, ** - p=<0.005.

Figure 4. E5.5 transplanted embryos show spread of GFP+ cells through the white matter of the spinal cord.

(A,B) Fluorescent stereoscopic examination revealed spread of GFP+ ENSCs from the transplantation site. (C) Schematic of the transplantation site and transverse and longitudinal sectioning planes used for analysis. (D) Co-staining of transverse sections with GFP and TuJ1 revealed transplanted ENSCs in neuronal rich regions. (E) In longitudinal sections, transplanted ENSCs formed bridging connections through the injury zone, between the anterior and posterior spinal cord tissue (E, arrow). In both transverse and longitudinal sections, GFP+ ENSC spread into the PNS through dorsal root ganglia (DRG, E). Numerous GFP+ projections extended from the transplanted neurosphere. FL – forelimb, HL – hindlimb, NT – neural tube, SN – spinal nerve, NC – notochord, DRG – dorsal root ganglia, WM – white matter, GM – grey matter. Scale bars: A = 3mm; B = 1mm; D,E = 500μm.

Figure 5. E7.5 transplanted embryos have a predominantly dorsal localisation of GFP+ cells to the spinal cord white matter and spread through the injury site.
(A,B) Fluorescent stereoscopic examination of embryos harvested at E7.5 revealed extensive cell spread from the transplantation site. (C) In transverse sections GFP+ cells were distributed in a 'halo' within the spinal cord white matter. Transplanted ENSCs had a preferential distribution around the dorsal spinal cord, with few cells located ventrally. (D) In longitudinal sections GFP+ cells formed bridging connections (arrow) between the anterior and posterior segments of the injured spinal cord. WM – white matter, GM – grey matter. Scale bars: A,B = 1mm; C,D = 500µm.

Figure 6. E9.5 transplanted embryos show spreading of GFP+ ENSCs through the white matter of the spinal cord and across the injury site.
(A) Transverse sections of E9.5 embryos showed GFP+ ENSCs localised almost exclusively to the dorsal spinal cord, with only occasional cells found more ventrally. (B) In longitudinal sections ENSCs formed bridging connections between anterior and posterior spinal cord tissues. The majority of cells localised to the white matter. WM – white matter, GM – grey matter. Scale bars: A,B = 500µm.

Figure 7. E13.5 transplanted embryos show extensive bridging of GFP+ ENSCs across the injury site and substantial anterior/posterior spread.
(A) Tiled images of longitudinally sectioned E13.5 embryos revealed the extent of ENSC spread along the anterior/posterior axis (maximum spread indicated by green arrows, white arrows highlight GFP+ cells). Solid and dashed lines in A show the approximate plane of transverse sections shown in B and C respectively, and the solid box indicates the higher magnification of the injury site shown in D. (B) Coronal section of the transplanted SC rostral to the transplantation site shows few GFP cells localised to the SC periphery, and some spread into the PNS. (C) Coronal sections within the injury zone reveal GFP+ cells within both white and grey matter. (D) Higher magnification of the injury zone demonstrates the extensive formation of GFP+ bridging strictures between the

anterior and posterior SC across the injury zone. Scale bars: A = 1000µm; B,C,D = 500µm.

Supplementary Figure 1. Cell fate and migration of transplanted ENSCs.
An analysis of cell fate revealed frequent TuJ1+ ENSCs (A) but no GFAP+ ENSCs (B). Transplanted ENSCs frequently aligned along the anterior/posterior axis (C). Quantification of GFP+ ENSC spread along the anterior-posterior axis across the three time points examined revealed a progressive increase in spread with increasing time post-transplant (D). Compared to an average spread of 996.3µm at E5.5, embryos harvested at E9.5 showed an average spread of 2931.4µm (n=3). Scale bars: B,C = 100µm. * - p=<0.05, ** - p=<0.005.

Supplementary Figure 2. Transplanted ENSC spinal cord localization. An analysis of HuC/D stained tissue showed a clear distinction between HuC/D+ endogenous neurons and transplanted GFP+ ENSCs can be clearly seen outside the grey matter, in the white matter (arrows), and in the injury zone (arrowhead). GM - grey matter, WM - white matter. Scale bar, 100µm.

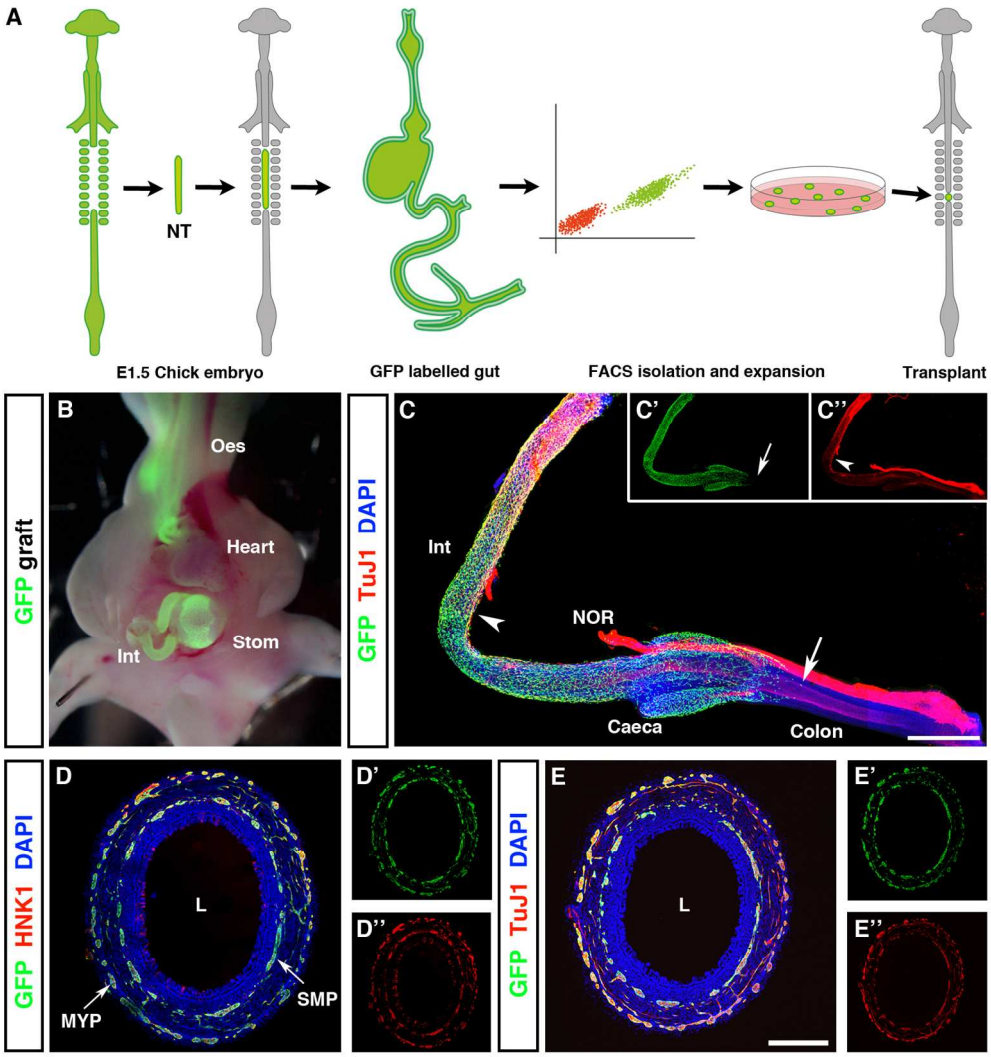

Figure 1. GFP chick intraspecies grafting efficiently labels the enteric nervous system of the gastrointestinal tract.

(A) Schematic representing chick embryo tissue grafting methodology. Neural tubes from the vagal region (adjacent to somites 1-7) of GFP+ E1.5 embryos were isolated and grafted into WT hosts in which the corresponding neural tube region was microsurgically ablated. Embryos developed for a further 12.5 days, at which point the intestines were harvested, stripped of mesentery, and dissociated into single cell suspension. GFP+ cells were isolated by FACS and expanded in culture to form GFP+ neurospheres for transplantation into E1.5 embryos. (B) Vagal neural tube grafting specifically labeled neural crest-derived tissues including the ENS of the GI tract. (C) At E6.5, GFP+ cells were observed along the gut, extending caudal to the caeca into the colon (C, arrow and C'). Following the migration wavefront TuJ1+/GFP+ cells were present (C, arrowhead and C''). (D, E) At E8.5, the GI tract was completely colonized by migrating neural crest cells. Transverse sections of the colon revealed the formation of GFP+ myenteric and submucosal plexuses. GFP+ cells co-expressed the neural crest cell marker HNK-1 (D'') and the neuronal marker TuJ1 (E''). NOR - nerve of Remak. Scale bars: C = 500μm; D,E = 250μm.

150x160mm (300 x 300 DPI)

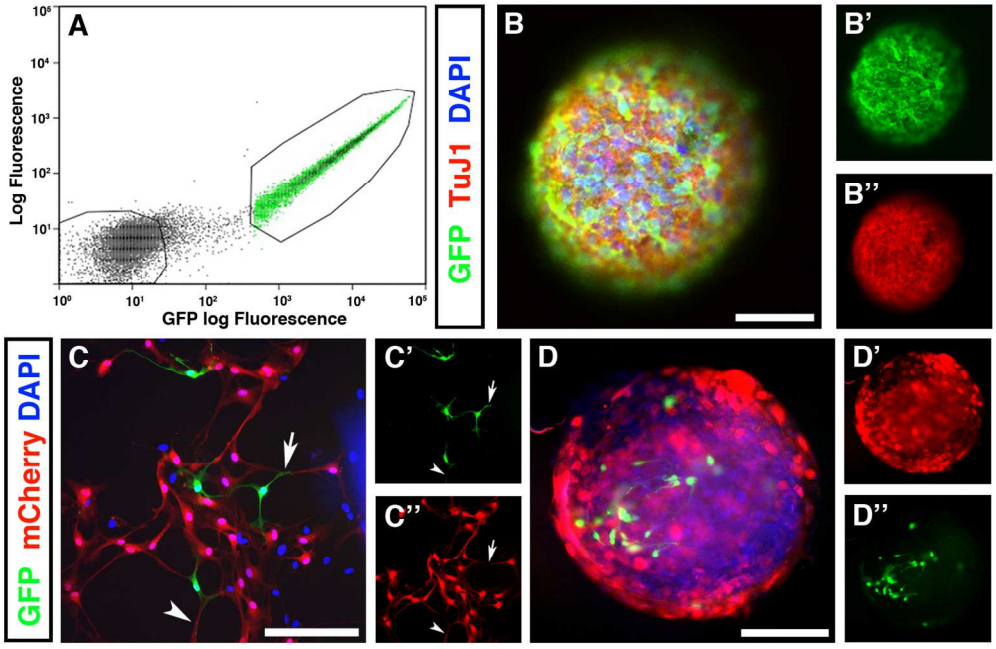

Figure 2. GFP+ enteric neural crest-derived cells form neurospheres and interconnections with CNS-derived cells in vitro.
After GFP tissue grafting, embryos were harvested at E14 and the gastrointestinal tract removed. (A) Gut tissues were dissociated into single cell suspension and sorted based on GFP expression and size. GFP negative populations were collected and cultured as controls. (B) Following FACS isolation, GFP+ graft-derived cells formed free-floating neurospheres after 1-2 weeks in culture. The majority of cells within neurospheres were immunopositive for the neuronal marker TuJ1 (B'). (C) GFP+ neural crest-derived cells were co-cultured with spinal cord (SC)-derived cells (labeled with an mCherry lentiviral construct). C' and C'' show higher magnification selections of C. (D) After several days in culture SC-derived cells (red, D') and ENS-derived GFP+ cells (D'') aggregated to form mixed-population neurospheres. Scale bars: B,C = 50μm; D = 100μm.

150x97mm (300 x 300 DPI)

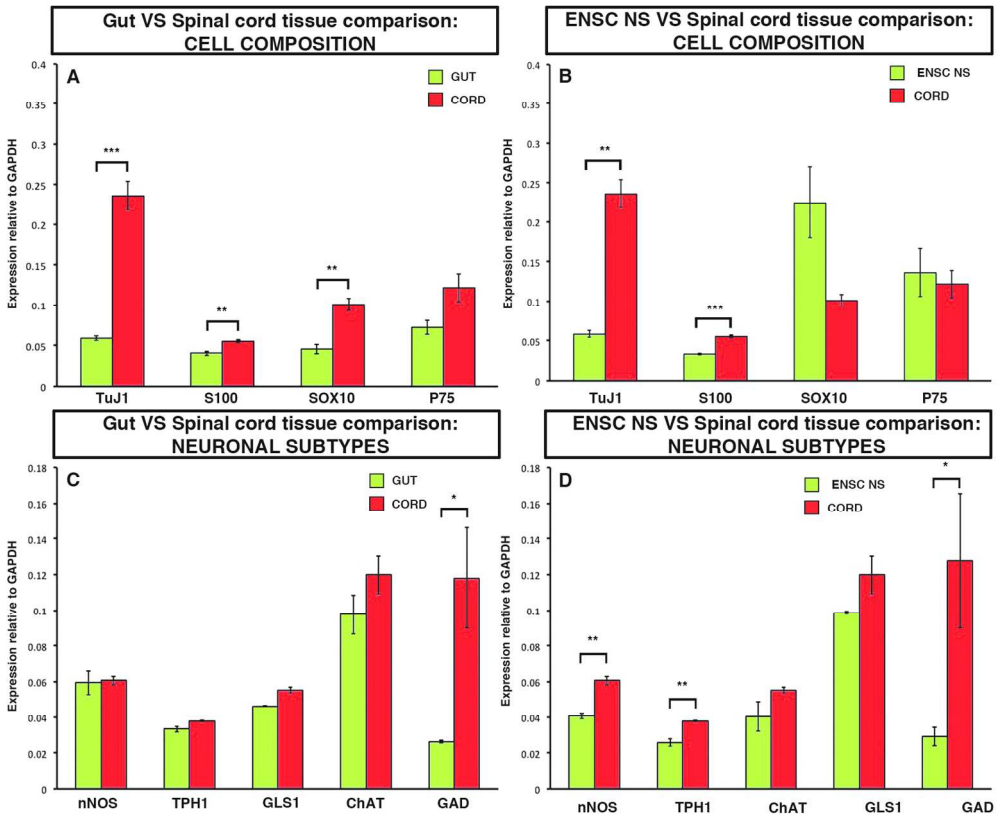

Figure 3. Cultured enteric neural crest-derived cells and whole SC samples express common neuroglial markers.

(A) Uncultured gut and SC tissues were analysed by qRT-PCR to determine relative expression levels of the neurosphere markers. TuJ1 (pan neuronal marker), S100 (glia), Sox10 (progenitor/stem cells) and the neural crest marker p75. (B) Expression levels of the neurosphere markers were assessed in cultured ENS-derived neurospheres and compared with expression in the SC. (C) Expression levels of specific neuronal subtypes were compared between uncultured gut and SC samples, including nNOS (NO), TPH1 (serotonin), GLS1 (glutamine) and ChAT (acetylcholine) and GAD (GABA) (D). The expression levels of these neuronal subtype markers were compared between ENS-derived neurosphere cultures and uncultured SC samples. nNOS, TPH1, GLS1, GAD n=3, ChAT n=2. * - p=<0.05, ** - p=<0.005.

146x119mm (300 x 300 DPI)

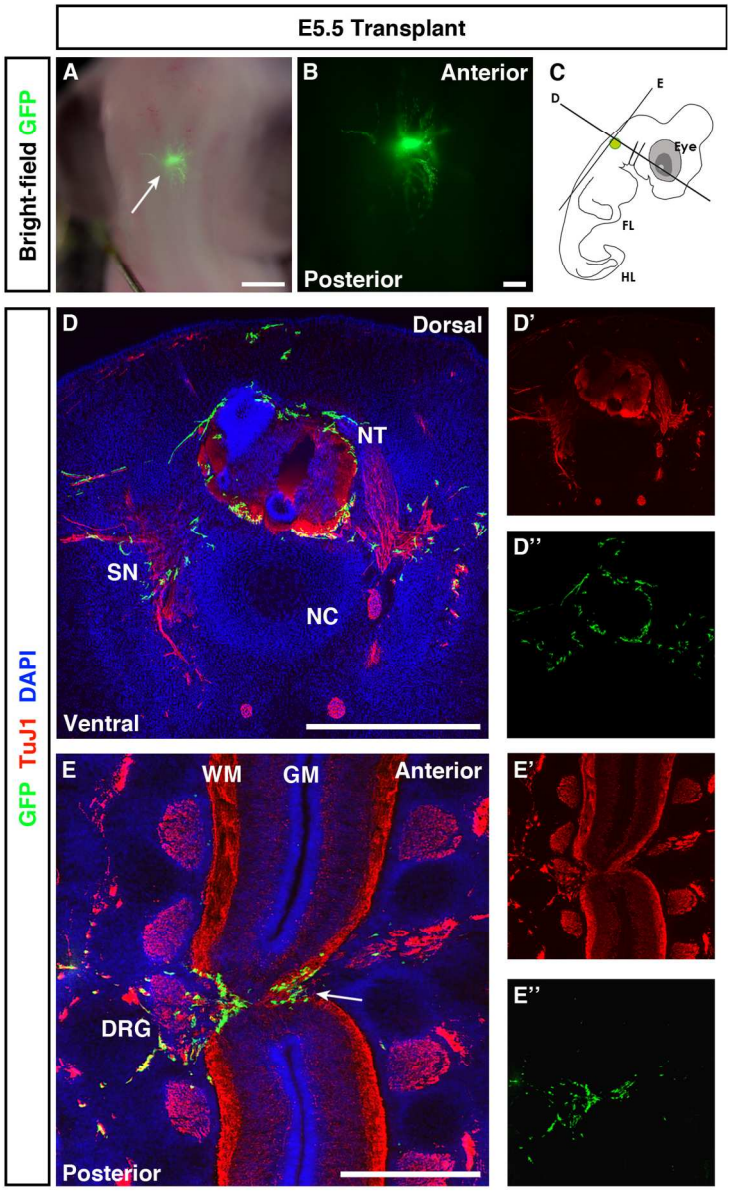

Figure 4. E5.5 transplanted embryos show spread of GFP+ cells through the white matter of the spinal cord. (A,B) Fluorescent stereoscopic examination revealed spread of GFP+ ENSCs from the transplantation site. (C) Schematic of the transplantation site and transverse and longitudinal sectioning planes used for analysis. (D) Co-staining of transverse sections with GFP and TuJ1 revealed transplanted ENSCs in neuronal rich regions. (E) In longitudinal sections, transplanted ENSCs formed bridging connections through the injury zone, between the anterior and posterior spinal cord tissue (E, arrow). In both transverse and longitudinal sections, GFP+ ENSC spread into the PNS through dorsal root ganglia (DRG, E). Numerous GFP+ projections extended from the transplanted neurosphere. FL – forelimb, HL – hindlimb, NT – neural tube, SN – spinal nerve, NC – notochord, DRG – dorsal root ganglia, WM – white matter, GM – grey matter. Scale bars: A = 3mm; B = 1mm; D,E = 500μm.

114x187mm (300 x 300 DPI)

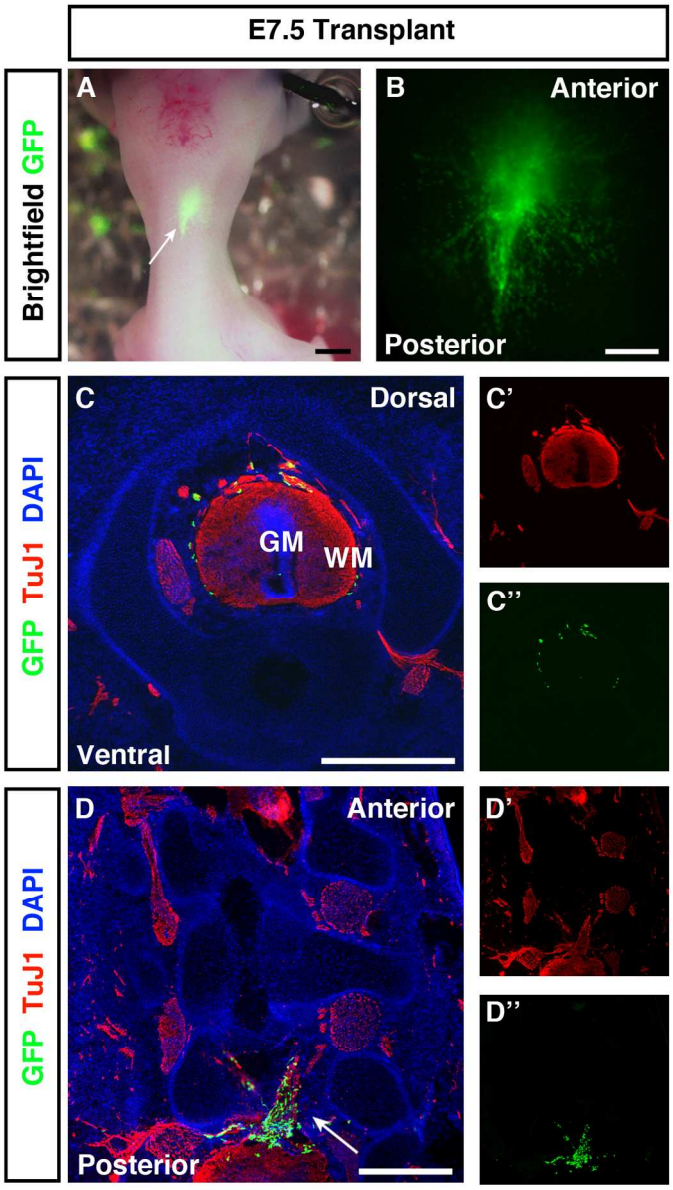

Figure 5. E7.5 transplanted embryos have a predominantly dorsal localisation of GFP+ cells to the spinal cord white matter and spread through the injury site.
(A,B) Fluorescent stereoscopic examination of embryos harvested at E7.5 revealed extensive cell spread from the transplantation site. (C) In transverse sections GFP+ cells were distributed in a 'halo' within the spinal cord white matter. Transplanted ENSCs had a preferential distribution around the dorsal spinal cord, with few cells located ventrally. (D) In longitudinal sections GFP+ cells formed bridging connections (arrow) between the anterior and posterior segments of the injured spinal cord. WM – white matter, GM – grey matter. Scale bars: A,B = 1mm; C,D = 500µm.

114x198mm (300 x 300 DPI)

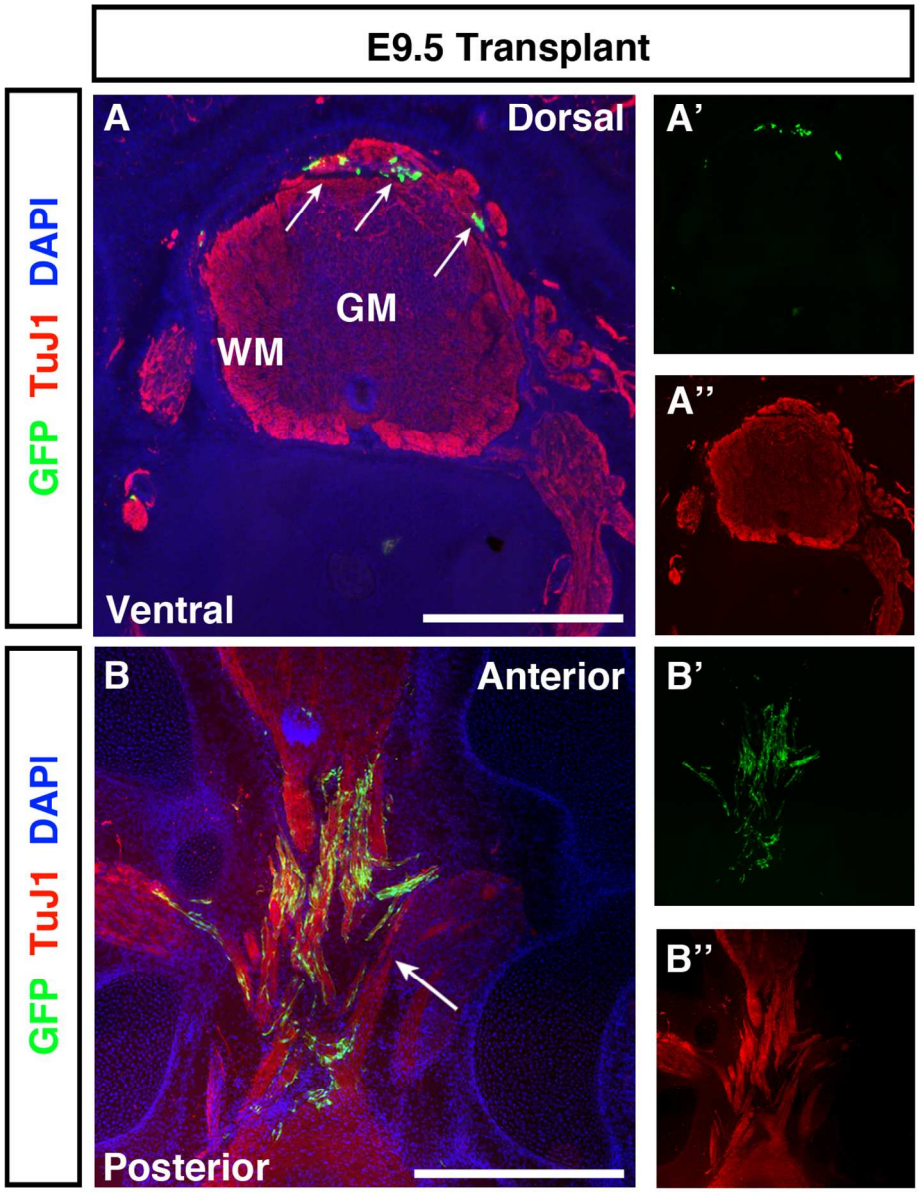

Figure 6. E9.5 transplanted embryos show spreading of GFP+ ENSCs through the white matter of the spinal cord and across the injury site.
(A) Transverse sections of E9.5 embryos showed GFP+ ENSCs localised almost exclusively to the dorsal spinal cord, with only occasional cells found more ventrally. (B) In longitudinal sections ENSCs formed bridging connections between anterior and posterior spinal cord tissues. The majority of cells localised to the white matter. WM – white matter, GM – grey matter. Scale bars: A,B = 500μm.

114x145mm (300 x 300 DPI)

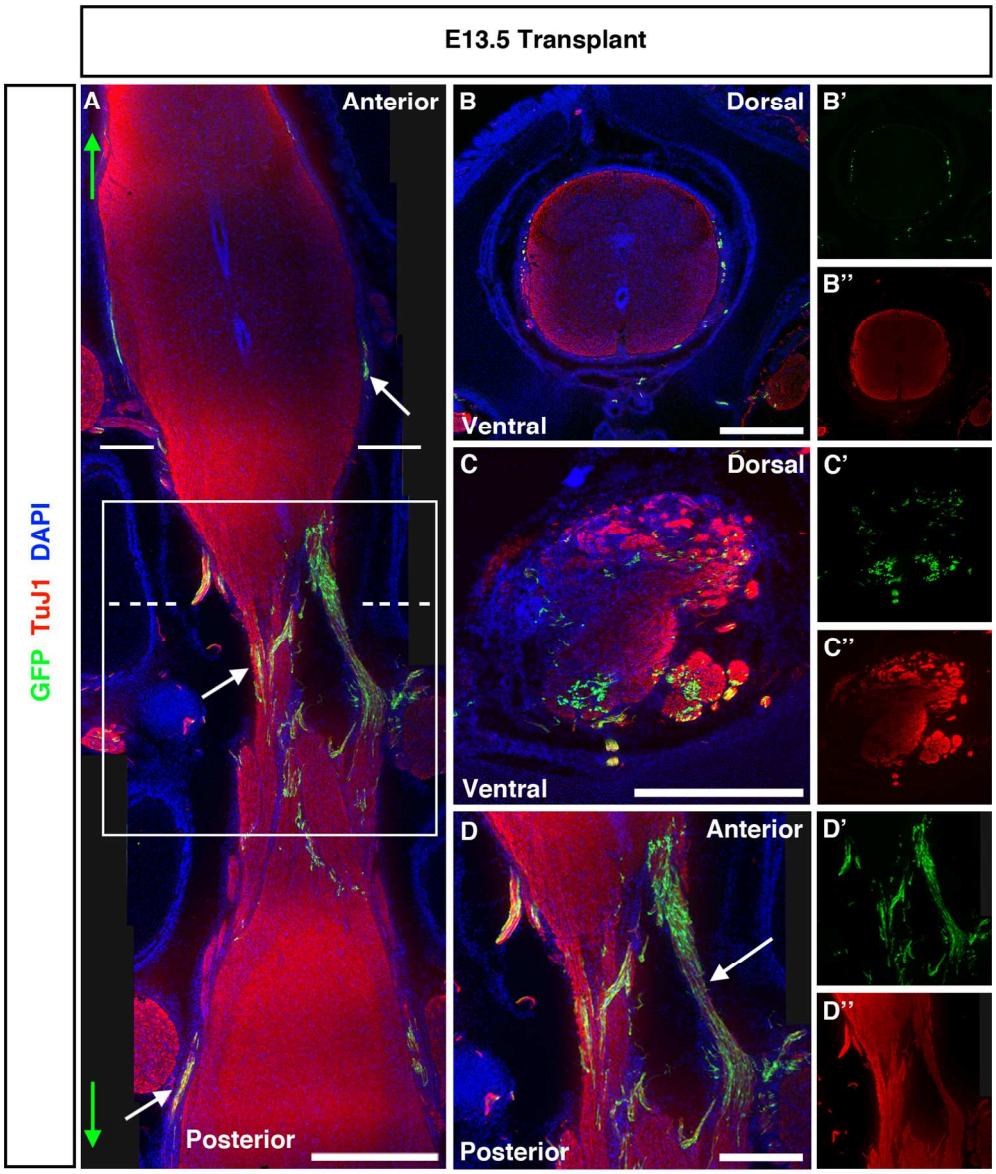

Figure 7. E13.5 transplanted embryos show extensive bridging of GFP+ ENSCs across the injury site and substantial anterior/posterior spread.
(A) Tiled images of longitudinally sectioned E13.5 embryos revealed the extent of ENSC spread along the anterior/posterior axis (maximum spread indicated by green arrows, white arrows highlight GFP+ cells). Solid and dashed lines in A show the approximate plane of transverse sections shown in B and C respectively, and the solid box indicates the higher magnification of the injury site shown in D. (B) Coronal section of the transplanted SC rostral to the transplantation site shows few GFP cells localised to the SC periphery, and some spread into the PNS. (C) Coronal sections within the injury zone reveal GFP+ cells within both white and grey matter. (D) Higher magnification of the injury zone demonstrates the extensive formation of GFP+ bridging strictures between the anterior and posterior SC across the injury zone. Scale bars: A = 1000μm; B,C,D = 500μm.

140x165mm (300 x 300 DPI)

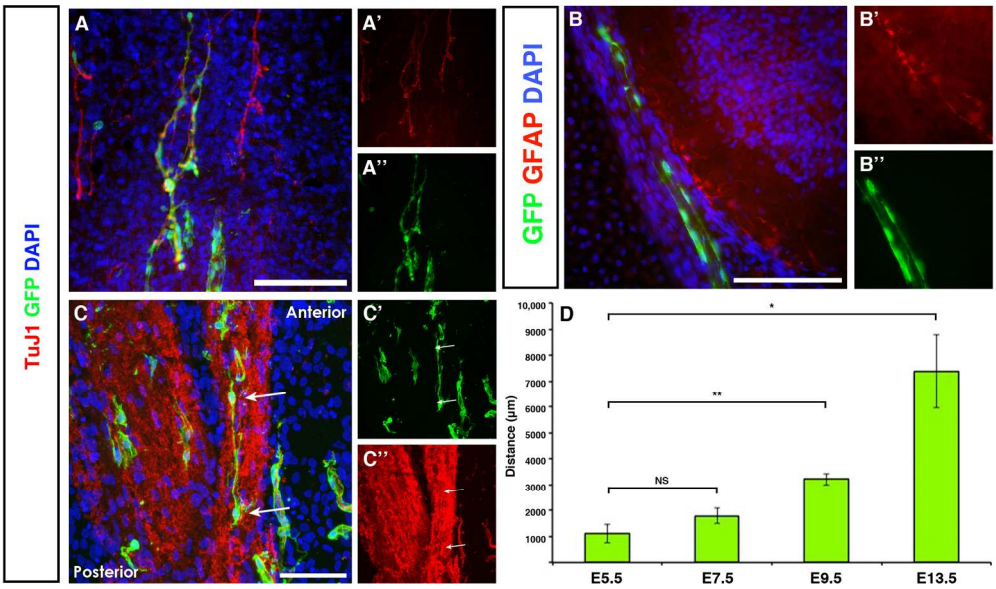

Supplementary Figure 1. Cell fate and migration of transplanted ENSCs.
An analysis of cell fate revealed frequent TuJ1+ ENSCs (A) but no GFAP+ ENSCs (B). Transplanted ENSCs frequently aligned along the anterior/posterior axis (C). Quantification of GFP+ ENSC spread along the anterior-posterior axis across the three time points examined revealed a progressive increase in spread with increasing time post-transplant (D). Compared to an average spread of 996.3µm at E5.5, embryos harvested at E9.5 showed an average spread of 2931.4µm (n=3). Scale bars: B,C = 100µm. * - p=<0.05, ** - p=<0.005.

177x103mm (300 x 300 DPI)

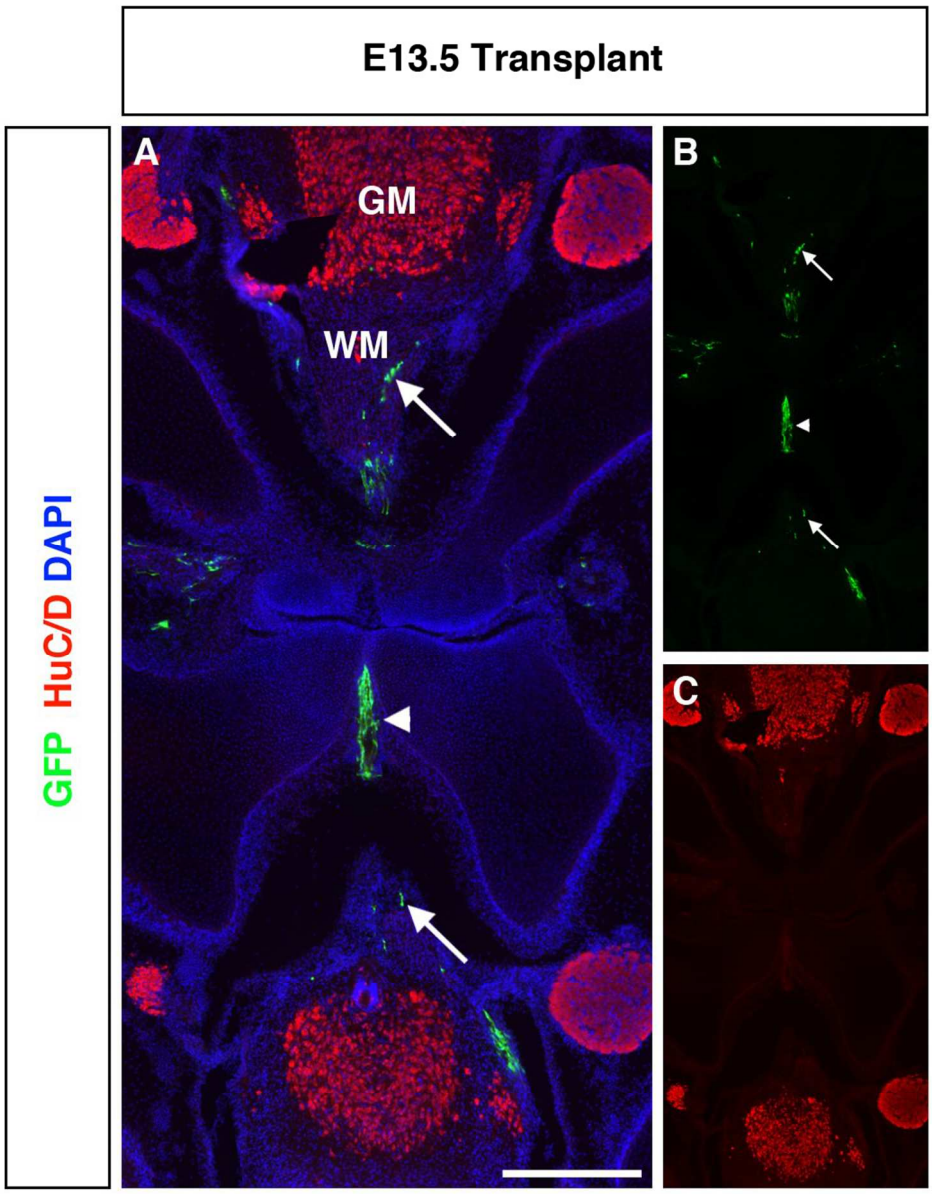

Supplementary Figure 2. Transplanted ENSC spinal cord localization. An analysis of HuC/D stained tissue showed a clear distinction between HuC/D+ endogenous neurons and transplanted GFP+ ENSCs can be clearly seen outside the grey matter, in the white matter (arrows), and in the injury zone (arrowhead). GM - grey matter, WM - white matter. Scale bar, 100μm.

88x113mm (300 x 300 DPI)